JOURNAL OF MATERIALS SCIENCE 31 (1996) 4939–4944

Microstructural and chemical stability of Y–ZrO_2 reinforced β″-alumina in molten sodium sulfide and sulfur

D. C. C. LAM*, K. KUSAKARI
Inorganic Materials Section, The Third Materials Department, Hitachi Research Laboratory, Hitachi, Ltd, 1-1 Omika-cho, 7-chome, Hitachi-shi, Ibaraki-ken 319-12, Japan

The stability of β″-alumina reinforced with 10 vol % of tetragonal partially stabilized 3 mol % Y_2O_3–ZrO_2 (3Y–ZrO_2) and with 10 vol % of cubic 8 mol % Y_2O_3–ZrO_2 (8Y–ZrO_2) in molten sulfur or molten Na_2S_4 has been examined using scanning electron microscopy (SEM) X-ray diffraction (XRD) and electron probe microanalysis (EPMA) both before and after immersion at 350 °C. Tetragonal partially stabilized 3 mol % Y_2O_3–ZrO_2 was destabilized when reinforced into β″-alumina and immersed in molten Na_2S_4. Destabilization without incorporation into β″-alumina or using molten S as the immersion medium was minor. EPMA analyses indicated that the presence of β″-alumina enhanced zirconia destabilization in that β″-alumina can react with the molten corrodants to form corrosion products which are known corrosion agents for the leaching of Y_2O_3 from partially stabilized 3Y–ZrO_2. From XRD analyses, changing from partially stabilized 3Y–ZrO_2 to cubic 8Y–ZrO_2 in the composite increased resistance against phase destabilization. EPMA analyses revealed that the depletion was almost halted for cubic 8Y–ZrO_2 suggesting that the change in the zirconia phase used had reduced the chemical reactivity between Y_2O_3 and the corrodants. In order to avoid depletion destabilization of zirconia in β″-alumina, corrosion resistance can be increased by reducing chemical reactivity by using fully stabilizing zirconia. In addition, partially stabilized tetragonal zirconia may still be considered for use if a less reactive stabilizer such as CeO_2 is used.

1. Introduction

NaS batteries have been considered for a long time as candidates for secondary energy storage for load levelling in power generation and for use as the power source in electric vehicles [1, 2]. During the operation of an NaS battery at temperatures between 300–400 °C, Na ions pass through the β″-alumina tube wall which acts as both a Na ion-conducting electrolyte and also as a separator for molten sodium on one side and Na_2S_x on the other. Under these operating conditions, β″-alumina has been known to suffer thermomechanical failure owing to Joule heating and thermal mismatch strains and also electrical failure owing to Na penetration across the electrolyte [1, 3]. To improve both thermomechanical and electrical failure resistance, partially stabilized Y_2O_3–ZrO_2 has been added to β″-alumina to increase both the strength and the critical current for Na penetration [4–7]. However, the strength of partially stabilized Y_2O_3–ZrO_2 has been known to degrade at elevated temperatures in electronegatively corrosive environments such as Na_2SO_4 molten salts [8–10]. The immersion and operation of an Y_2O_3–ZrO_2/β″-alumina composite in a molten Na_2S_x may suffer similar degradation.

In the present study, the stability of Li_2O (0.74 wt %) stabilized β″-alumina ($Na_2O \cdot y\ Al_2O_3$; $y = 6.58$) reinforced with 10 vol % of partially stabilized tetragonal 3 mol % Y_2O_3–ZrO_2 (3Y–ZrO_2) and with cubic 8 mol % Y_2O_3–ZrO_2 (8Y–ZrO_2) in molten sulfur and molten Na_2S_4 are examined after immersion at 350 °C. Their stability will be compared with the corrosion stability of monolithic β″-alumina (shortened to β″), monolithic partially stabilized tetragonal 3 mol % Y_2O_3–ZrO_2 (3Y–ZrO_2) and monolithic cubic 8 mol % Y_2O_3–ZrO_2 (8Y–ZrO_2) before and after immersion. By comparing the corrosion and phase stability, the effect of β″ on Y–ZrO_2 stability, the influence of partially stabilized tetragonal and fully stabilized cubic ZrO_2 and the effect of Na_2S_4 and S corrosion environments can be determined. The various effects will be discussed with respect to known monolithic β″ and monolithic Y–ZrO_2 corrosion behaviour reported in the literature.

* *Present address*: Department of Mechanical Engineering, Hong Kong University of Science and Technology, Clear Water Bay, Kowloon, Hong Kong.

0022–2461

2. Experimental procedure

Two different β″-alumina composites with 10 vol % of either 3Y–ZrO_2 (0.3 μm TZ-3YS and TZ-8Y, Tosoh Chemical, Tokyo, Japan) or 8Y–ZrO_2 were made via spray drying. Measured quantities of high molecular weight organics (2 wt % of polyvinyl butyral, MW = 35,000 Wako Chemical, Japan, 1 wt % of liquid paraffin, Wako Chemical, Japan, 0.25 wt % polyethylene imine, MW = 70,000, Wako Chemical, Japan, wt % based on total ceramic wt) sufficient for 500 ml of 32 vol % solid loading slurry were mixed in ethanol and ultrasonicated (Model US-1200, Nihonseiki Kaisha Ltd., Japan) for 15 min. Then, measured quantities of 3Y–ZrO_2 or 8Y–ZrO_2 were slowly added into the prepared solvent and ultrasonicated for 10 min at high power. Afterwards, measured quantities of β″-alumina were slowly stirred into the slurry and ultrasonicated for 20 min forming a thick, but fluid 500 ml slurry. Then the slurry was magnetically stirred for 2 h and was ultrasonicated once more for 20 min before spray drying. The spray drying was done in a small spray dryer (Model SD-2. Tokyo Rikakikai Co., Japan) at an inlet temperature of 75 °C, outlet temperature of 50 °C and spraying pressure of 1.38 kPa. After spray drying, the granules were collected in a double capped plastic bottle for storage.

From these granules, 2 g were weighed, poured into a double action metal die (50 mm × 5 mm cavity) and uniaxially pressed (Model R-213, Riken Seiki Co., Japan) at 300 MPa producing prismatic bars with a thickness varying from 3.1–3.5 mm. After pressing, the bars were equilibriated in a dessicator for 24 h or more. The organics in the bars were pyrolysed off by heating the bars from room temperature at a ramp rate of 50 °C per h to 800 °C with a hold for an hour and then heated at 300 °C per h to more than 1500 °C and held for more than 5 min (Exact conditions are proprietary), then ramped at 300 °C per h to 1400 °C, held for more than 2 h and then cooled to room temperature at 300 °C per h. After sintering, the bars were ground and polished for immersion. In addition to the composites, disks of monolithic β″, 3Y–ZrO_2 and 8Y–ZrO_2 were pressed from ungranulated raw powder and sintered using the same sintering schedule.

The polished bars and disks were then tied with wires onto a stainless steel cage, suspended in the middle of a Na_2S_4 filled Al_2O_3 crucible inside a stainless steel cylinder and enclosed within a closed atmospherically controlled testing cell (Fig. 1). The air was evacuated from the cell and was backfilled with argon gas. The cylinder was heated and held at 350 °C so that the Na_2S_4 melted and the bars were immersed in molten Na_2S_4 in closed conditions. After one week of immersion, the cell was cooled and the bars now encased in the solidified sulfide were removed from container. The outer portion of the sulfide encrustation was then removed with water and the inner encrustation was then removed by immersion in methanol. Then the samples were washed gently and ultrasonicated with methanol to remove the remaining Na_2S_4 on the surface. The entire procedure was then repeated for another set of samples immersed in molten sulfur. After immersion, the as-polished

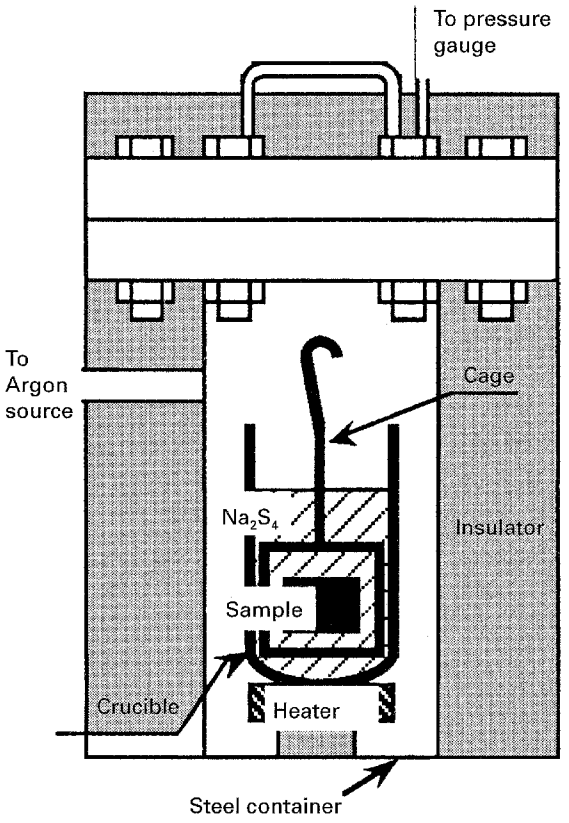

Figure 1 Schematic of closed corrosion testing cell.

samples and immersed samples were examined using scanning electron microscopy (SEM) (Model S-570 SEM, Hitachi Ltd, Japan) and X-ray diffraction (XRD) (Model RU-200 with Cu$K\alpha$ radiation Rigaku Ltd., Japan). The fraction of monoclinic phase was calculated from the relative areas underneath the diffraction profiles of $(111)_M$, $(11\bar{1})_M$ and $(111)_{T,C}$ as described by Garvie and Nicholson [11]. The surface chemical changes, specifically the mole ratios of Y/(Y + Zr) and Al/Na before and after immersion were examined using electron probe micro analysis (EPMA) (EPMA Model 1560 with Sun SPARC workstation, Shimadzu, Japan). For statistical accuracy, a probe size of 100 μm was used so that a typical sampling would include ~250 Y–ZrO_2 particles (~2 μm dia., Fig. 2) in the composite. With the electron probe set on a fixed sample area, Y and Zr signals were collected using a pentaerythritol (PET) collector while the Al and Na counts were collected using a rubidium acid phthalate (RAP) collector. The peak positions and their respective integration limits are detailed in Table I. As can be seen from this table, all the peaks, particularly those for element 39 Y and the neighbouring element 40 Zr have no overlap. Consequently, the total signal (counts) from an element does not require any peak deconvolution software which normally introduce appreciable systematic errors into the measured results when the elemental content is low and signals are overlapped.

3. Results and discussions

XRD spectra for a 3Y–ZrO_2/β″ composite before and after immersion in Na_2S_4 and S are shown in Fig. 3.

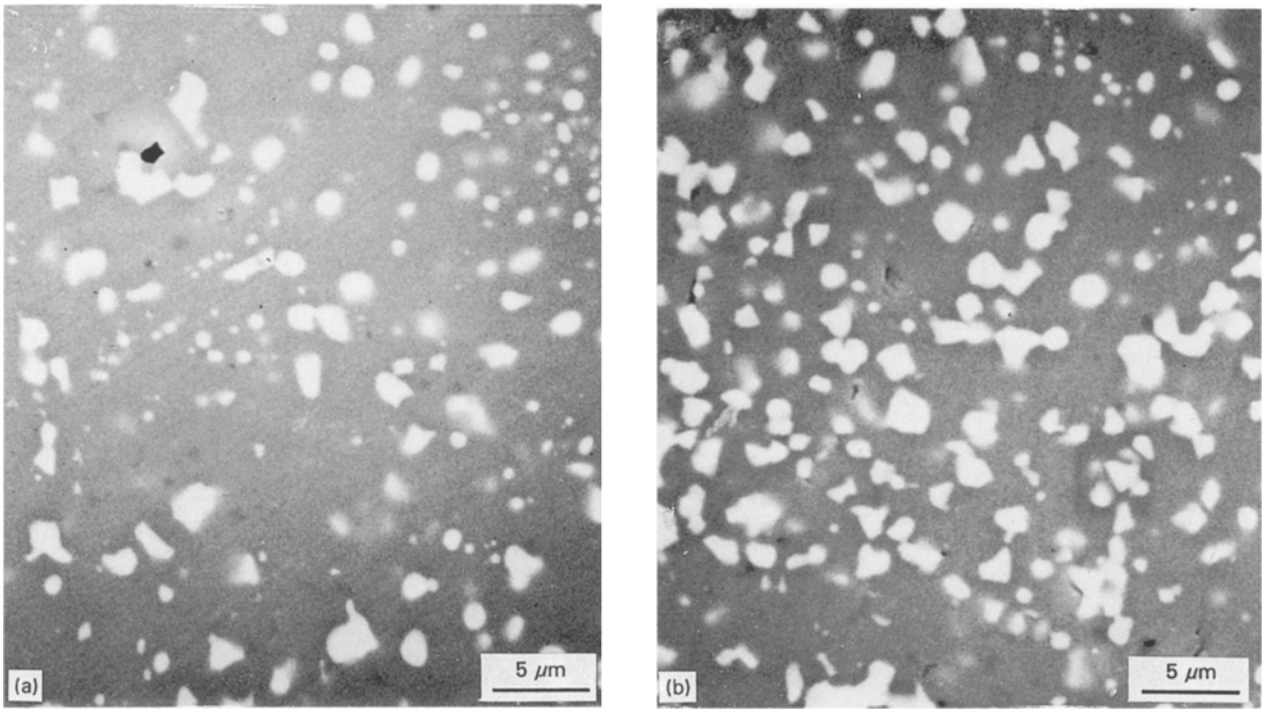

Figure 2 SEM micrographs of (a) 8Y–ZrO_2/β″-alumina before immersion and (b) after immersion in Na_2S_4 at 2000× magnification showing similar surfaces before and after immersion.

TABLE I EPMA conditions

	Max. limit[a] (nm)	Peak (nm)	Min. limit (nm)	Sampling time(s)	Min. total counts
Y (L_α)	0.65488	0.64440	0.63488	200[b]	> 6000
Zr (L_α)	0.61705	0.60648	0.59705	50	> 18000
Al (K_α)	0.88393	0.83313	0.78393	50	> 740000
Na (K_α)	1.29101	1.19042	1.09101	50	> 130000

[a] Maximum and minimum limits of intensity integration are set by software algorithm at the point when signal decayed to background level.
[b] Sampling time is increased to increase accuracy for minor element.

After immersion in Na_2S_4, the X-ray data indicated that the ~27% of tetragonal phased 3Y–ZrO_2 in the 3Y–ZrO_2/β″ composite had been destabilized and transformed into the monoclinic phase. EPMA analyses revealed that the destabilization was accompanied by depletion of Y_2O_3 from 3 mol% to 2.28 mol% in the sample immersed in Na_2S_4 (Fig. 4). Comparatively, the amount of monoclinic phase in the sample immersed in sulfur was minor (~3.3%) as was the decrease in stabilizer content from 3 mol% to 2.9 mol%, which is within experimental error. From these EPMA and XRD data, the Y_2O_3 depletion and accompanying phase transformation suggest that molten Na_2S_4 destabilized 3Y–ZrO_2 in 3Y–ZrO_2/β″ by depleting the Y_2O_3 stabilizer and also that Na_2S_4 was more corrosive than molten S.

Similar 3Y–ZrO_2 destabilization via Y_2O_3 depletion had been observed previously when Y_2O_3 was leached from monolithic 3Y–ZrO_2 when treated between 150–400 °C in a hydrothermal environment at moderate temperature [8–10]. However, EPMA (Fig. 3) and X-ray data for monolithic 3Y–ZrO_2 without β″ (Fig. 5) indicated that Na_2S_4 immersion did not produce a similar Y_2O_3 depletion or transformation to that observed in the 3Y–ZrO_2/β″ case. The difference in behaviour between the monolithic and composite cases indicate that the reaction between Na_2S_4 and Y_2O_3 in 3Y–ZrO_2 is limited without the presence of β″ which appears to be a necessary component in the leaching of Y_2O_3 by Na_2S_4.

β″-alumina corrosion by Na_2S_x and S has been studied by Liu and DeJonghe both experimentally and from the viewpoint of thermodynamic calculations [12]. From their Auger electron analyses of the corroded surface and thermodynamic calculations, they concluded that the thermodynamically stable products from Na_2S_x and S corrosion of β″ were NaOH and sulfates such as $Na_2(SO_4)_3$, $NaAl(SO_4)_3$, $Al_2(SO_4)_3$ and $NaHSO_4$ via reactions

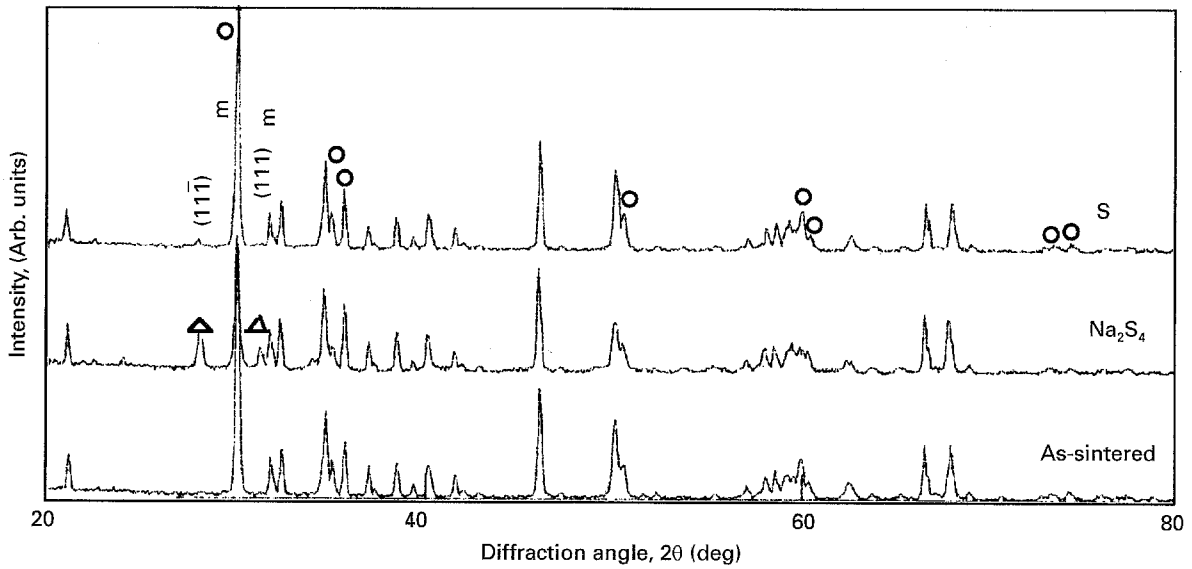

Figure 3 X-ray diffraction spectra of 3Y–ZrO_2/β″ before and after immersion in Na_2S_4 and S. (Δ) Monoclinic $(1\,1\,1)_M$ and $(11\bar{1})_M$ peaks and (○) tetragonal peaks are identified directly on the spectra. All other unmarked peaks are β″-alumina peaks. Immersion in molten Na_2S_4 transformed 27% of the tetragonal zirconia into monoclinic zirconia. Immersion in molten S transformed ~3.3% into monoclinic zirconia.

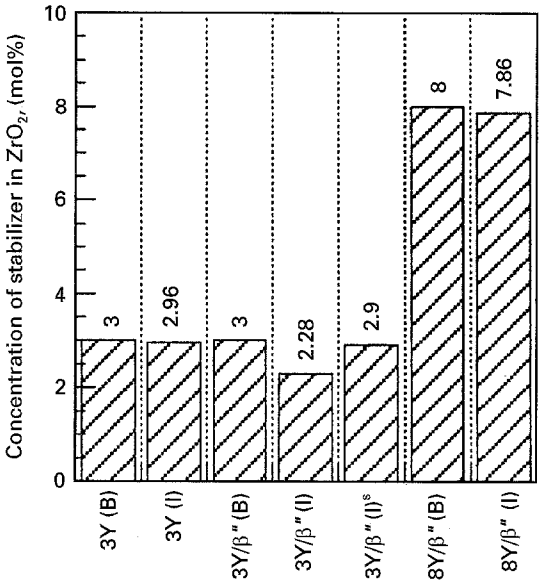

Figure 4 EPMA measurement of Y stabilizer content (error ± 3%) before and after immersion for one week. (B) denotes samples before immersion and (I) denotes immersed samples. All immersed samples were immersed in molten Na_2S_4 unless superscripted by ^{s} which denotes immersion in molten sulfur.

such as:

$$Na_2O{\cdot}yAl_2O_{3(s)} + 4zS_{(1)}$$

$$\Leftrightarrow (1-z)Na_2O{\cdot}yAl_2O_{3(s)} + \frac{3z}{4}Na_2S_{5(1)}$$

$$+ \frac{z}{4}Na_2(SO_4)_{3(s,l)} \quad (1)$$

This resulted in active corrosive pitting of β″ in the case of molten Na_2S_4 and passive precipitate deposition (non-ionic molten S has more limited solubility for ionic salts) on the surface of the polished β″ in the case of molten sulfur [12]. EPMA analysis of monolithic β″ revealed that the corrosion caused a decrease in the Al/Na ratio from 6.58 to 5.74, for the as-sintered and corroded β″ respectively (Fig. 6). The change in surface Al/Na ratio indicated that β″ in the present study did react with molten Na_2S_4 such that sulfates and hydroxides were probably formed owing to the presence of β″.

Sulfates and hydroxides from β″ corrosion are known depletion agents of Y_2O_3 in 3Y–ZrO_2 [8–10, 13–15]. The depletion typically follows reactions such as

$$3Al_2(SO_4)_{3(s,l)} + 4Y_2O_{3(s)} + 12Na_2S_{x(l)}$$

$$\Leftrightarrow 12Na_2S_{x-1(l)} + 4Y_2(SO_4)_{3(s,l)} + 3Al_2S_{3(s,l)} \quad (2a)$$

$$3Na_2(SO_4)_{3(s,l)} + 4Y_2O_{3(s)} + 12Na_2S_{x(l)}$$

$$\Leftrightarrow 12Na_2S_{x-1(l)} + 4Y_2(SO_4)_{3(s,l)} + 3Na_2S_{3(s,l)} \quad (2b)$$

in which β″ reaction products are consumed. The consumption of the corrosion products would tend to accelerate β″ corrosion. The accelerated β″ corrosion in 3Y–ZrO_2/β″ as reflected in a larger change in the Al/Na ratio was confirmed by the large decrease of the Al/Na mole ratio from as-sintered 6.58 to 2.9 for 3Y–ZrO_2/β″ (Fig. 6). Clearly, β″ played a role in the corrosion of the 3Y–ZrO_2/β″ composite in that it provided the corrosive species of sulfates and hydroxides and due to this the depletion of Y_2O_3 in 3Y–ZrO_2/β″ from 3 mol % down to 2.26 mol % was enabled (Fig. 4).

Since this leaching of Y_2O_3 is the cause for the destabilization then increasing the Y_2O_3 content from 3 mol % to 8 mol % and changing from partially stablized tetragonal to the fully stabilized cubic phase may improve the resistance to destabilization. XRD studies on an 8Y–ZrO_2/β″ composite showed no monoclinic phase after immersion in either S or Na_2S_4 (Fig. 7). EPMA data (Fig. 4) indicated that the Y content in 8Y–ZrO_2 decreased slightly to 7.86 mol % whilst the Al/Na ratio decreased to 5.24 (Fig. 6). The

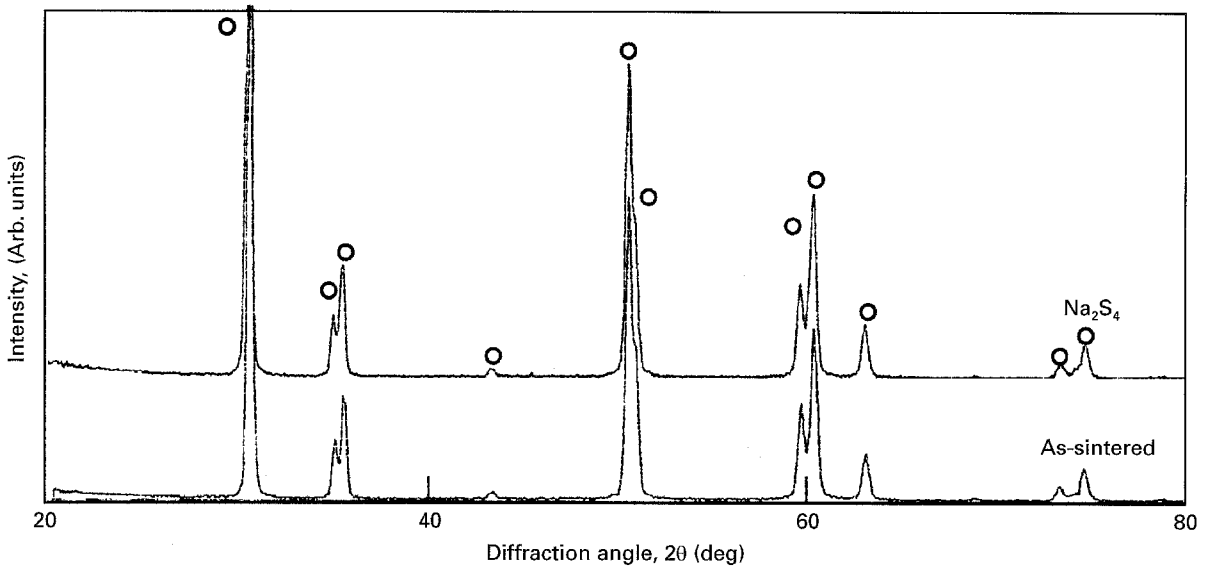

Figure 5 X-ray diffraction spectra of tetragonal 3Y–ZrO_2 before and after immersion in Na_2S_4. All peaks have been identified as belonging to (O) tetragonal zirconia. The diffraction pattern shows no monoclinic $(1\ 1\ 1)_M$ or $(11\bar{1})_M$ peaks indicating that no phase change occurred therefore pure 3Y–ZrO_2 is stable in Na_2S_4.

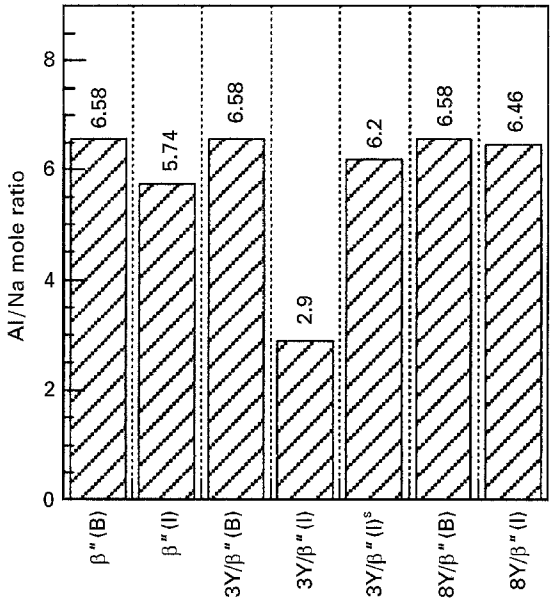

Figure 6 EPMA measurement of the Al/Na ratio (error ± 3%) before and after immersion for one week. (B) denotes samples before immersion and (I) denotes immersed samples. All immersed samples were immersed in molten Na_2S_4 unless superscripted by ^{s} which denotes immersion in molten sulfur.

demonstrably slower depletion suggested that the driving force for Y_2O_3 leaching was decreased owing to the change from partially stabilized tetragonal to the stable cubic Y–ZrO_2 phase. If phase stability had no effect, then the Y content should have decreased to a level comparable to that observed in the case for 3Y–ZrO_2 ($\Delta Y_2O_3 = 0.72$ mol %). Thus, the increased stability of 8Y–ZrO_2/β″ can be attributed primarily to the change from partially stabilized tetragonal phase to stable cubic phase. XRD and EPMA results for 8Y–ZrO_2/β″ immersed in molten S gave similar results indicating that 8Y–ZrO_2/β″ is stable in both Na_2S_4 and S.

The corrosion of β″-alumina ceramics by Na_2S_x is typically most severe at cracks, defects and grain junctions [12]. This corrosion behaviour is similar to that which has been observed for α-alumina which exhibited preferential corrosion at grain junctions when immersed in concentrated NaOH solutions at temperatures above 150 °C [16]. The corrosion, as measured by weight loss, can be decreased by half if the α-alumina is reinforced by 20 mol % of partially stabilized tetragonal 12Ce–ZrO_2 (3Y–ZrO_2 is not stable in such alkaline hydrothermal conditions) presumably by strengthening the corrosion resistance of the grain junction. Similarly, the more stable Al/Na ratio of 8Y–ZrO_2/β″ (Fig. 6) and the unpitted surface observed for 8Y–ZrO_2/β″ after immersion (Fig. 2) indicate that stable 8Y–ZrO_2 at β″ grain junctions may have increased the corrosion resistance of β″ in Na_2S_4. Of course, longer term tests are needed to confirm the results.

4. Conclusion

The stability of β″ alumina reinforced with 10 vol % of partially stabilized tetragonal 3 mol % Y_2O_3–ZrO_2 or with cubic 8 mol % Y_2O_3–ZrO_2 in molten sulfur and molten Na_2S_4 has been examined after immersion at 350 °C. Partially stabilized tetragonal 3 mol % Y_2O_3–ZrO_2 was destabilized when reinforced into β″-alumina and immersed in molten Na_2S_4. EPMA analyses indicate that the 3 mol % Y_2O_3–ZrO_2 destabilization was accompanied by leaching of Y_2O_3 from 3Y–ZrO_2/β″-alumina. Without the presence of the β″-phase transformation did not occur and Y_2O_3 content remained relatively constant. From both XRD and EPMA analyses, cubic 8 mol % Y–ZrO_2/β″-alumina was more stable than 3 mol % Y–ZrO_2/β″- alumina. Changing from partially stabilized tetragonal 3 mol % Y–ZrO_2/β″-alumina to cubic 8 mol % Y–ZrO_2/β″-alumina appears to have stopped the Y leaching and improved β″-alumina resistance to Na_2S_4 corrosion. The leaching of Y_2O_3 from Y–ZrO_2 depended on the presence

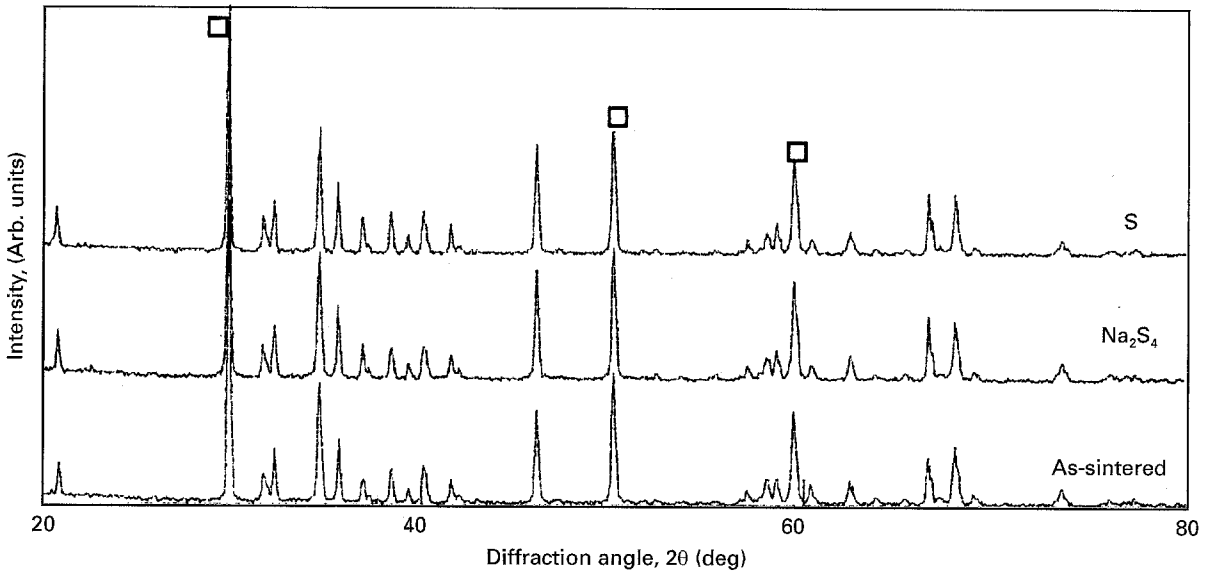

Figure 7 X-ray diffraction spectra of 8Y–ZrO_2/β″ before and after immersion in Na_2S_4 and S at 350 °C for one week. The diffraction pattern shows only cubic zirconia marked as (Δ) and β″-alumina peaks (unmarked). No monoclinic $(1\,1\,1)_M$ or $(11\bar{1})_M$ peaks were detected indicating that no phase change occurred.

of (i) β″-alumina which produced the corrosion agents, (ii) a thermodynamically and kinetically active corrosion medium such as Na_2S_4, and (iii) a reactive form of Y_2O_3 as in 3 mol % Y_2O_3–ZrO_2. The absence of one of the three conditions has been shown to decrease or halt destabilization of the Y–ZrO_2.

Acknowledgement

We gratefully acknowledge the experimental help of Shin-ya Imano and Yoshiteru Chiba and also discussions with Kozo Sakamoto, Dr. Yukio Saito and Dr. Ken Takahashi, all of Hitachi Research Laboratory.

References

1. J. L. SUDWORTH in "NaS Batteries", edited by J. L. Sudworth and A. R. Tilley, (Pergamon Press, London, 1986) p. 7.
2. STAFF. *Automotive Engng* [9] (1992) 17.
3. R. O. ANSELL, *J. Mater. Sci.* **21** (1986) 365.
4. D. J. GREEN, *ibid.* **20** (1985) 2639.
5. L. VISWANATHAN, Y. IKUMA and A. V. VIRKAR, *ibid.* **18** (1983) 109.
6. F. F. LANGE, B. I. DAVIS and R. O. RAYLEIGH, *J. Amer. Ceram. Soc.* **66** (1983) C-50.
7. J. G. P. BINNER and R. STEVENS, *J. Mater. Sci.* **20** (1985) 3119.
8. K. KOBAYASHI, H. KUWAJIMA and T. MASAKI, *Solid State Ionics* **3/4** (1981) 489.
9. J. J. SWAB and G. L. LEATHERMAN, *J. Eur. Ceram. Soc.* **5** (1989) 333.
10. T. SATO and M. SHIMADA, *J. Amer. Ceram. Soc.* **68** (1985) 356.
11. R. C. GARVIE and P. S. NICHOLSON, *ibid.* **55** (1972) 303.
12. M. LIU and L. C. DEJONGHE, *J. Electrochem. Soc.* **135** (1988) 741.
13. R. L. JONES, S. R. JONES and C. E. WILLIAMS, *ibid.* **132** (1985) 1498.
14. J. C. HAMILTON and A. S. NAGELBERG, *J. Amer. Ceram. Soc.* **67** (1984) 686.
15. A. S. NAGELBERG, *J. Electrochem. Soc.* **132** (1985) 2502.
16. T. SATO, S. SATO and A. OKUWAKI, *Corrosion Sci.* **33** (1992) 581.

Received 8 September 1994
and accepted 13 February 1996